Journal of Network Intelligence
Taiwan Ubiquitous Information
 ISSN 2414-8105
Volume **9**, Number **3**, August **2024**

Digital Copyright Protection of Images Based on Invasive Weed Optimisation Algorithm

Xia Zhou*
Information College
Furong College, Hunan University of Science and Arts, Changde 41500, P. R. China
intercomputer2023@163.com

Andrea Santos
College of Engineering
University of San Juan Letran, Intramuros Manila 1002, Philippines
va8938@163.com

*Corresponding author: Xia Zhou
Received November 4, 2023, revised February 15, 2024, accepted April 22, 2024.

Abstract. *Research on digital copyright protection for images provides digital media platforms and social media with important tools to ensure that users do not infringe on the intellectual property rights of others when sharing and distributing digital images. This contributes to a fairer and more legitimate digital ecosystem that encourages creators to actively share their work while protecting their creative output. Therefore, the digital copyright protection technique for images with invasive weed algorithm is proposed. Firstly, the principles and characteristics of human visual system are introduced, and the perceptual characteristics of colour images and the conversion relationship between colour spaces are analysed. Then, the proposed watermarking algorithm is described in detail, in which the watermarked image is disrupted to increase the security of the algorithm. An invasive weed optimisation algorithm is used to select the appropriate embedding strength to embed the watermark information into the carrier image wavelet transform coefficients to balance the algorithm robustness and invisibility. The optimal solution of embedding strength is obtained by seed dispersal and weed multiple competitive optimisation. Finally, experiments were conducted using MATLAB software and the results were analysed. Experimental results show that compared with the common particle swarm optimization and differential evolution algorithm, the proposed method not only improves the applicability of the algorithm, but also shows strong robustness to noise attacks, compression and geometric attacks such as rotation, shearing and translation on the basis of ensuring the invisibility of the algorithm.*
Keywords: invasive weed optimisation; fitness; digital watermarking; copyright protection; colour images

---

1. **Introduction.** Digital copyright protection refers to a range of technical, legal and regulatory measures designed to ensure that the intellectual property rights of creators or owners of digital media content are legally protected against unauthorised copying, distribution, modification or other infringement [1, 2]. This includes a wide range of digital content such as text, images, audio, video, etc. The main goal of digital copyright protection is to prevent piracy and infringement in order to encourage creators to create more content and to ensure that they receive a fair reward for their creative endeavours.

Digital copyright protection can be achieved by a variety of methods, including digital watermarking [3], encryption [4], access control [5], digital rights management systems

(DRM) [6], and legal action [7]. These methods can help protect digital content from unauthorised copying and distribution while allowing legitimate users to gain access and usage rights. Digital rights protection is an important part of protecting intellectual property rights in the digital age, helping to safeguard the rights and interests of creators and content providers while promoting innovation and sustainable development of digital content.

Digital watermarking technology through a certain algorithm will contain a certain significance of the logo information embedded in the multimedia content, for the content itself does not hinder its normal use, embedded watermark information can be the serial number of the owner of the digitised product, the product's company logo or this paper with a special meaning of the information, pictures, etc. [8, 9]. Watermark information is generally not easy to be noticed, noticed, only through a professional detector or computer software can be detected, and only the use of the corresponding watermark extraction algorithm can be hidden watermark information can be extracted more completely. Digital watermarking technology has a wide range of application prospects, in the realisation of digital multimedia works copyright protection [10], data authentication or tampering tips [11], data content integrity authentication [12], as well as broadcasting facilities monitoring [13] and other aspects play an increasingly important role.

With the in-depth study of related watermarking technologies, optimisation-based digital watermarking algorithms have been popularised, and optimisation-based algorithms represented by ant colony algorithms, particle swarm optimisation algorithms, genetic algorithms, neural network algorithms, and differential evolution algorithms have been successfully applied to the field of digital watermarking research. Therefore, the research objective of this work is to design novel digital watermarking optimisation algorithms in order to further improve the usefulness of digital copyright protection of images.

1.1. **Related Work.** The process of designing a digital watermarking scheme belongs to a kind of optimality seeking solution problem [14]. The research on digital watermarking based on bionic optimisation algorithms is evolving and some significant progress has been made. Bionic optimization algorithms are computational algorithms inspired by the evolution and behaviour of organisms in nature, and they have been used to improve the robustness, stealth and security of digital watermarking.

Giri and Bashir [15] proposed a new wavelet transform based digital watermarking algorithm for colour images using the principle of bionic optimization [16] to optimize the digital watermarking algorithm by combining the principle of bionic optimization. Salimi et al. [17] proposed the use of differential evolution algorithm to improve the transparency of SVD-based digital watermarking algorithm by using the optimal value obtained by the differential evolution algorithm, which can then make up for the visual loss of the image caused by embedding watermarking by using SVD. Thakkar et al. [18] proposed a new digital watermarking algorithm with the use of SVD and singular value decomposition to improve the transparency of digital watermarking. Thakkar and Srivastava [18] proposed an adaptive digital image watermarking algorithm based on differential evolution and Contourlet transform.

Zheng et al. [19] used particle swarm optimization (PSO) algorithm to optimize the watermarking technique based on image or audio, which can improve the performance of the watermarking algorithm to a certain extent. Cui et al. [20] proposed a digital watermarking algorithm for medical images using differential evolution optimization. Zhuang et al. [21] proposed a reversible digital watermarking algorithm for the protection of the electronic medical records of patients in hospitals from being illegally accessed by third parties using differential evolution algorithm with medical images as the watermarking carrier. Bose and Maity [22] proposed a DWT-SVD digital watermarking optimisation algorithm based on differential evolution using medical images as the watermarking carrier. Later on, an improvement of this watermarking algorithm is proposed to adaptively take the values of the parameters involved in the operation of the differential evolution algorithm, which reduces the complexity of manually adjusting the parameters.

Invasive Weed Optimization (IWO) is an ecologically inspired optimisation algorithm for solving various optimisation problems. It works similar to the process of weed growth and invasion in ecology. In invasive weed optimisation algorithms, solutions compete and invade to find the optimal solution. Kumar et al. [23] introduced the application of the IWO algorithm to the N-queen problem. The researchers compared the algorithm with traditional heuristics and evaluated the performance of the invasive weed optimisation algorithm in solving this classical combinatorial optimisation problem. The results show that the algorithm achieves competitive results in the N-queen problem. Sivananthamaitrey and Kumar [24] proposed to apply the IWO algorithm to find the optimal embedding location to protect colour image watermarks from attacks. The experimental results show that the method successfully embeds the watermark information while maintaining the quality of the image. Yue and Zhang [25] proposed to apply the IWO algorithm to the problem of image segmentation. Experimental results show that the method achieves good segmentation results on several benchmark image datasets.

1.2. **Motivation and contribution.** The main advantages of IWO over other bionic optimisation algorithms (e.g. PSO and DE) are its adaptivity, diversity, simplicity, parallelism and better global search capability.IWO simulates the growth and aggression behaviour of plant populations, and is highly exploratory and robust for multidimensional optimisation problems [26, 27].

The advantages of applying IWO to the field of digital watermarking lie in its adaptivity, robustness and global search capability in terms of digital watermark embedding position and strength. IWO helps to determine the optimal watermark embedding strategy to ensure that the digital watermark remains stable in the face of attacks and transformations, while being difficult to be detected by unauthorised users, improving the quality and stealthiness of the digital watermark. This makes IWO a promising algorithm choice for digital watermarking applications in areas such as intellectual property protection, content authentication and copyright protection. Therefore, to further improve the utility of digital copyright protection for images, this work proposes an invasive weed optimisation algorithm based digital copyright protection technique for images.

The main innovations and contributions of this work include:

(1) The principles and characteristics of the human visual system are introduced, and the perceptual characteristics of colour images and the conversion relationship between colour spaces are analysed. Then, the proposed watermarking algorithm is described in detail, in which the watermarked image is scrambled to increase the security of the algorithm.

(2) The colour image is used as the carrier image of the watermarking algorithm, and the appropriate watermark embedding strength is selected based on the IWO algorithm by combining the HVS characteristics. It not only increases the applicability of the algorithm, but also shows strong robustness to noise attacks, compression, and geometric attacks such as rotation, shear, and translation on the basis of ensuring certain algorithmic invisibility.

2. **Principles of the IWO algorithm.**

2.1. **Biological background of the IWO algorithm.** Weeds are plants that grow in places that are not valuable for human survival but occupy places where human production activities take place, and these plants are generally not cultivated by humans. There are more than 300,000 species of plants that have been identified and named by scientists globally, and about 8,000 of them are recognised as weeds, and they are divided into different species according to their appearance, growth characteristics, and reproduction modes.

In general, plants known as weeds share some common characteristics, such as diversity of dispersal modes, superior reproductive capacity and regeneration, excellent resistance to stress, and high photosynthetic efficiency and short growth cycles. When these weeds grow in agricultural fields, they compete with crops for nutrients, water, sunlight, space and other resources in the soil. From the beginning of human farming activities, humans have been struggling with weeds, in addition to the common artificial weed control, mechanical weed control and drug weed control, as well as biological weed control, ecological weed control and integrated weed control and other new weed control methods. However, thousands of years of history have proved that weeds are always a winner, because today, weeds are still present in all corners of the earth, and with the renewal of human weeding methods, weeds have also evolved stronger resistance and environmental adaptability.

Generally speaking, weed invasion needs to go through the following process: firstly, weed seeds enter the farmland through natural diffusion, and try their best to adapt to the surrounding environment, with the help of crop growth gaps, waiting for the opportunity to grow and take root, in order to fight for their own necessary living space. Then in the process of growth, constantly competing with the surrounding crops and other weeds, for their own growth for nutrients. Weeds that are more competitive have access to more nutrients and space to grow, and naturally produce more seeds as they mature, while less competitive weeds produce fewer seeds. The mature seeds are naturally shed and dispersed around the parent weed to become a new generation of weed seeds. Among the new generation of seeds, poorly adapted individuals are eliminated by the process of natural selection, leaving behind the well-adapted seeds that continue to grow and reproduce. After a few generations, the weed completely encroaches on the surrounding territory and becomes the new ruler.

2.2. **Mathematical description of the IWO algorithm.** The IWO algorithm is a commonly used evolutionary algorithm, and the flow of the IWO algorithm is described below in conjunction with Figure 1 [28].

The key idea of IWO algorithm is to simulate the spread and growth of weeds in the search space, and gradually optimize the fitness function by constantly updating the seed population to find the best solution. This algorithm is usually used for continuous optimization problems, but it can also be modified to adapt to different types of problems. The larger the fitness value the more number of seeds are sown by the individual. The mathematical description of the common parameters of the IWO algorithm is shown in Table 1.

The reproductive rate of invaders is calculated according to their fitness and the distance between adjacent seeds. Generally, invaders with higher adaptability and nearby seeds with closer distance will have higher reproduction rate. The relationship between fitness and seeds is as follows:

$$S_{\text{num}} = \text{floor}\left[\frac{f(X_i) - F_{\min}}{F_{\max} - F_{\min}}(S_{\max} - S_{\min}) + S_{\min}\right] \tag{1}$$

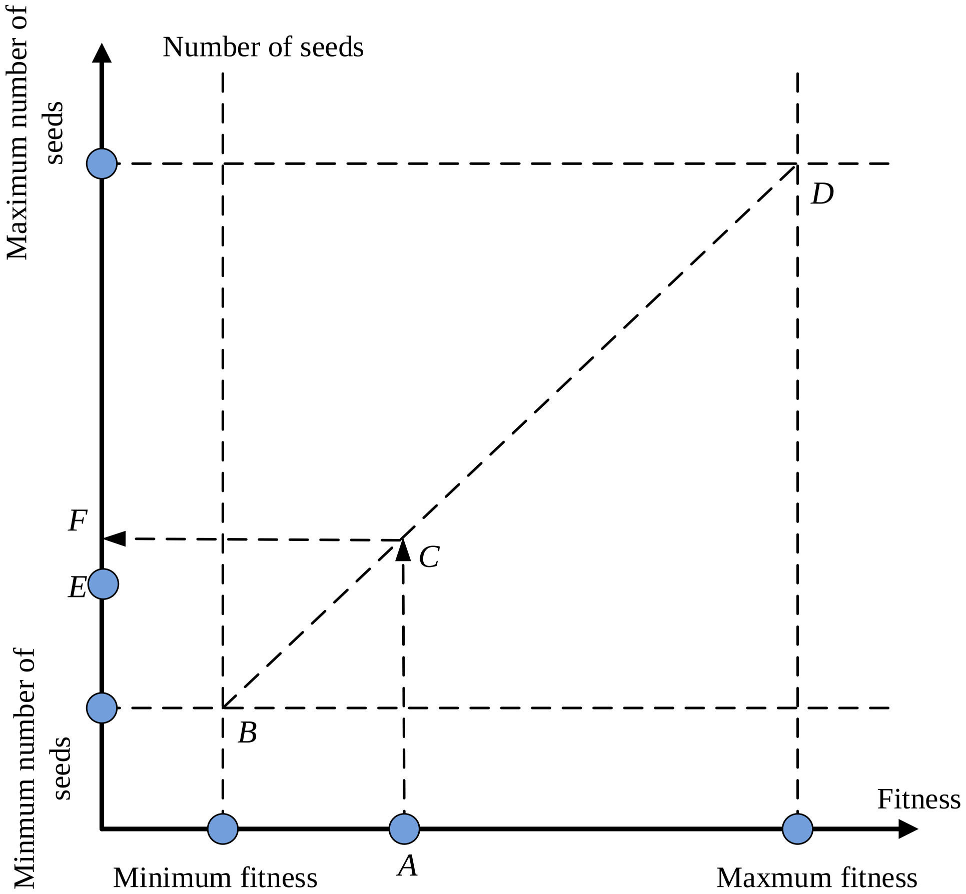

Figure 1. Schematic diagram of mathematical description of IWO algorithm

Table 1. Mathematical description of common variables of IWO algorithm

variant	**Variable Description**
Adaptation Minimum	$F_{\max}$
Adaptation maximum	$F_{\min}$
Minimum number of seeds	$S_{\min}$
Maximum number of seeds	$S_{\max}$
Maximum population size	$P_{\max}$
Initial stock size	$P_{\min}$

When the fitness value is in negative feedback with the number of seeds, then Equation (2) is used instead of Equation (1).

$$S_{\text{num}} = \text{floor}\left[\frac{F_{\max} - f(X_i)}{F_{\max} - F_{\min}}(S_{\max} - S_{\min}) + S_{\min}\right] \tag{2}$$

where floor() denotes the rounding function [29].

In IWO algorithm, seeds usually represent potential solutions to problems, and their positions are usually represented by numerical values. These values may represent the characteristics or parameter values of the solution. In some cases, the parameters of the solution must be integers, such as some discrete problems or specific optimization problems.

After calculating the number of seeds according to Equation (1) or Equation (2), as follows:

$$X_{i,s} = X_i + N(0, \sigma_{\text{iter}}^2), S_{\min} \leq s \leq S_{\max} \tag{3}$$

where $X_{i,s}$ denotes the distribution of seeds after reproduction of the first i seed, centered on X_i and σ_{iter} is calculated:

$$\sigma_{\text{iter}} = \sigma_{\text{final}} + \left(\frac{\sigma_{\max} - \text{iter}}{\text{iter}_{\max}}\right)^w (\sigma_{\text{initial}} - \sigma_{\text{final}}) \tag{4}$$

For each seed, input it into the objective function, and calculate the value of the objective function according to Equation (3) and Equation (4). This value is the fitness value of the seed. In IWO algorithm, the objective function is usually used to minimize the problem, so the lower the fitness value, the better the solution. You can specify in advance the maximum number of iterations that the algorithm will run. Once this limit is reached, the algorithm will stop. Or we can set a target fitness value, and once the fitness value of any seed reaches or approaches this value, the algorithm can be terminated early.

Due to the rapid reproduction of the population, after a few generations, the maximum population size will be reached $m_{\max}$. After all the weeds in the current iteration have reproduced according to the size of the fitness value, the newborn population and the parent population will be sorted together according to the fitness value, and the first $m_{\max}$ weed individuals with smaller fitness values will be saved to participate in the next round of growth and reproduction, while all the other individuals with small fitness values will be eliminated.

2.3. **Characteristics of the IWO algorithm.** A large number of applications for IWO have demonstrated the development potential of the IWO algorithm.

(1) Reproduction rule based on fitness value.In the IWO algorithm, the seed reproduction process depends on the size of the fitness value, the larger the fitness value represents the stronger the environmental adaptability, the more offspring are allowed to reproduce. The smaller the fitness value, the less adaptable the environment is, and the fewer offspring are allowed to reproduce. This mechanism fits well with the probabilistic and periodic nature followed by evolutionary algorithms and ensures the diversity of the population [30].

(2) Gentle competitive exclusion mechanism: In the IWO algorithm, when the number of seeds reaches the upper limit of environmental carrying capacity, instead of the conventional way of deleting the best individuals directly according to the fitness value, all the individuals are allowed to reproduce and spread out and then eliminated according to the fitness value. This elimination mechanism ensures that those individuals with lower fitness values in the population also have a certain chance to reproduce, thus increasing the diversity of the population and greatly reducing the possibility of the population falling into a local optimum earlier.

(3) Seed dispersal following normal distribution.In the IWO algorithm, weed seeds are dispersed around the parent following a zero-mean normal distribution, which allows the weed seeds to spread farther away from the parent at the beginning of the iteration.

3. Human visual models.

3.1. **Properties of the human visual model.** Human Visual System (HVS) is a very sophisticated image processing system, but the system still has many imperfections.

On the one hand, HVS has some visual redundancy characteristics, is less sensitive to some noise, and is less sensitive to textured regions of an image than to smooth and edge regions of an image. The human eye also cannot accurately recognise when the texture characteristics of an image are changed. On the other hand, HVS shows different brightness perception characteristics for different colours with the same background conditions, and has different sensitivities to different frequency domain regions of the image, and is less sensitive to high-frequency components of the image. Therefore, when designing the watermarking algorithm, it is important to pay attention to the carrier image involved in the algorithm as well as the brightness, texture, frequency domain and edge information of the watermarked image and other factors that are important to HVS.

The human visual system (HVS, Human Visual System) is a complex and sophisticated system with several key properties that can be analysed in two main parts [31]: perceptual and cognitive properties.

(1) Perceptual properties. The human visual system is capable of perceiving different wavelengths of light, including red, green and blue. The cone cells in our retina can distinguish between these colours, enabling us to see a rich variety of colours. This ability helps us to identify and distinguish between objects of different colours.HVS is very sensitive to contrast. We can perceive differences in light and dark between objects, which helps us to recognise edges and details in a scene. High contrast helps in highlighting objects and low contrast helps in blurring and softness. Humans have a wide field of vision, front and back. We can perceive and focus on multiple objects and areas in our field of view, although the central field of view has a higher resolution. Since we have two eyes, we are able to achieve stereoscopic vision, perceiving depth and three-dimensional space. This helps us to estimate the distance and position of objects.The HVS is able to sense the motion and speed of objects, which is important for tracking moving objects and navigation.

(2) Cognitive properties. The human brain has an excellent pattern recognition ability to recognise and understand a variety of complex patterns and shapes. This helps us to recognise objects, faces, words, etc. HVS tends to gaze and focus on specific areas of the visual field. Eye movement is the phenomenon where our eyes move rapidly to scan different areas. This helps us to focus and perceive more details. The human visual system is susceptible to optical and psychological illusions. This means that we may have false perceptions in certain situations, especially under the influence of certain conditions such as light, background, etc. HVS can help us recognise different objects, faces and other specific features, which is important for social interaction, object recognition and navigation.

3.2. **Perceptual properties of the human visual model for colour images.** The perceptual properties of the human visual model for colour images show excellent colour sensitivity and discrimination. Through the different types of cone cells in the retina, we are able to perceive various colours such as red, green and blue, and integrate this information in the brain, enabling us to observe the colourful world.

In addition, our visual system is very sensitive to contrast and is able to perceive changes in brightness and colour in different areas of an image, thus enabling us to distinguish between the outlines and details of objects. This ability of colour perception and contrast perception enables us to deeply understand and appreciate the subtleties of colour images, including colour differences between different objects and backgrounds, textures, changes in lighting, and overall image composition. These perceptual properties give us a high degree of sensitivity to colour images, enabling us to derive complex information from them and to make perceptions and decisions.

The RGB (red, green and blue) model has a number of limitations in its application to colour description of colour images. Firstly, the RGB model uses only three channels to represent colour information, whereas real-world colours are continuous and consist of a myriad of wavelengths and spectral components, and therefore cannot fully capture subtle colour differences. Secondly, the *RGB* model cannot handle the brightness and saturation information of colours, which means that it ignores the brightness and shades of colours when describing them. Finally, the *RGB* model is also unable to handle subjective differences in colour perception, as different people may perceive the same colour differently, and this subjectivity cannot be captured by the *RGB* model. Therefore, in order to describe the colours of colour images more accurately, more sophisticated colour models such as Lab colour space are required, which can represent the attributes of colours more comprehensively, including brightness, hue and saturation, to better meet the needs of human perception. Therefore, the *YIQ* colour space is used in this work.

The *YIQ* colour space belongs to the *NTSC* system and is mostly used for image communication, where Y represents the luminance component of an image and I and Q represent the colour components. Converting a colour image from the *RGB* format to *YIQ* separates the luminance component Y from I and Q in the image. In addition, the human eye shows less sensitivity to the Y component than the components I and Q. The linear transformation between *RGB* and *YIQ* is simple to compute and has better clustering. The relationship between *RGB* and *YIQ* colour space conversion is shown below:

$$\begin{bmatrix} Y \\ I \\ Q \end{bmatrix} = \begin{bmatrix} 0.299 & 0.587 & 0.114 \\ 0.596 & -0.275 & -0.321 \\ 0.212 & -0.523 & 0.311 \end{bmatrix} \cdot \begin{bmatrix} R \\ G \\ B \end{bmatrix} \tag{5}$$

$$\begin{bmatrix} R \\ G \\ B \end{bmatrix} = \begin{bmatrix} 1.0 & 0.956 & 0.620 \\ 1.0 & -0.272 & -0.647 \\ 1.0 & -1.108 & 1.703 \end{bmatrix} \cdot \begin{bmatrix} Y \\ I \\ Q \end{bmatrix} \tag{6}$$

Where R, G and B represent the luminance values of the red, green and blue channels respectively.

4. IWO-based digital copyright protection for colour images.

4.1. Watermark generation. In the watermark generation stage, Arnold disruption technology is mainly used to preprocess the watermark image to improve the security of the algorithm. In the watermark embedding and extraction process, DWT-SVD processing is applied to the carrier image to achieve the purpose of enhancing the robustness of the watermarking algorithm. The specific process is shown in Figure 2.

The embedding strength values for watermarks are taken empirically and are generally set as constants. In fact, the selection of embedding strength is adaptive according to the different images, which can be achieved by using the IWO algorithm. The watermark information is embedded and extracted according to the embedding intensity values of different frequency subbands of the original image. After the watermark is embedded, common algorithmic attacks are performed on the watermarked image, causing different degrees of distortion to the image according to various attack functions. This work combines the objective function involved in the IWO algorithm to achieve the optimisation of the watermarking algorithm. The objective function is closely related to the invisibility and robustness of the watermarking algorithm and its expression is shown below:

$$\text{Maximize} f = NC(W, W^*) + NC(I, I^*) \tag{7}$$

where W denotes the watermarked image, W^* denotes the extracted watermarked image, I denotes the original image, and I^* denotes the image containing the watermark.

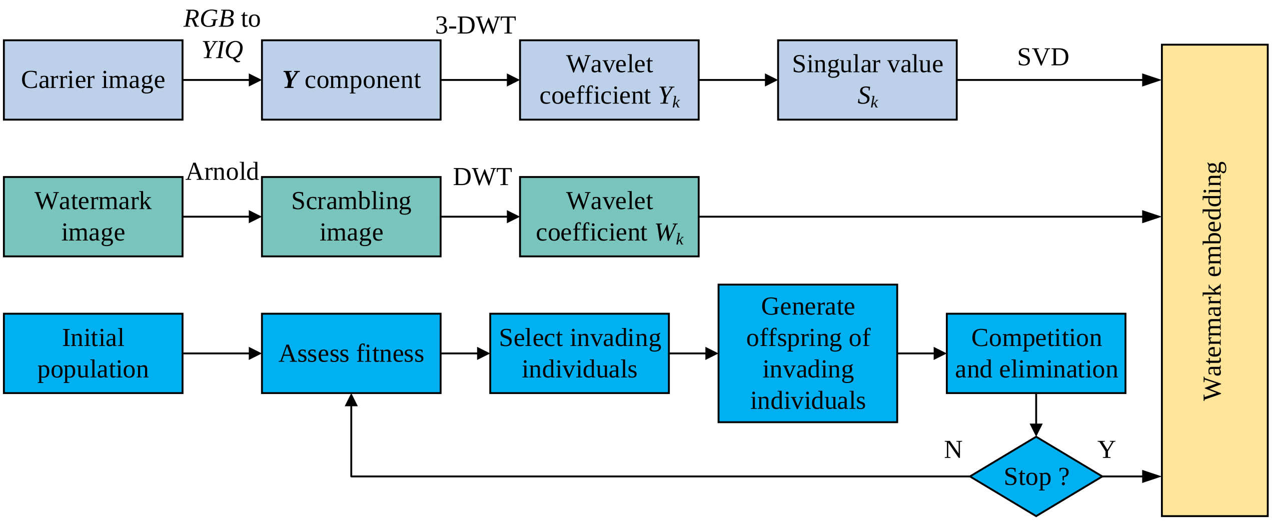

Figure 2. Watermark embedding process

Normalized Correlation (NC) denotes the normalized correlation coefficient, which reflects the similarity of the two images, and is an objective criterion for evaluating the effectiveness of watermark extraction.

The larger value of $NC(I, I^*)$ indicates that the more similar the original image is to the watermarked image containing watermark, i.e., the better the watermarking algorithm is hidden. The larger value of $NC(W, W^*)$ indicates that the more similar the watermarked image is to the extracted watermarked image, i.e., the better the robustness of the algorithm is. The definition of the NC function is shown below:

$$NC(X, \hat{X}) = \frac{\sum_i \sum_j X(i,j)\hat{X}(i,j)}{\sqrt{\sum_i \sum_j X(i,j)^2}\sqrt{\sum_i \sum_j \hat{X}(i,j)^2}} \tag{8}$$

where X denotes the original image (or watermarked image) and $\hat{X}$ denotes the watermarked image (or extracted watermarked image).

Three population individuals are arbitrarily selected for the diffusion operation, where the diffusion factor $F[0.4, 0.9]$ is obtained according to Equation (4). t denotes the maximum number of evolutionary generations of the IWO algorithm, and t denotes the current number of individual generations.

$$F = F_{\max} - (F_{\max} - F_{\min})\left(\frac{t}{T}\right)^2 \tag{9}$$

Reproduction produces new individuals for competitive evolution operations.

4.2. **Embedding algorithm for watermarking.** Colour space conversion of carrier image $\mathbf{A}$ to RGB format to YIQ format.

Then, the $\mathbf{Y}$ component of the YIQ space is extracted and a three-level DWT is performed to obtain four different frequency components, including a low-frequency approximation subband as well as three high-frequency detail subbands $\mathbf{Y}_k$.

According to Equation (10), the four subbands $\mathbf{Y}_k$ obtained above are subjected to SVD decomposition to find the corresponding singular values $\mathbf{S}_k$.

$$\mathbf{Y}_k = \mathbf{U}_k\mathbf{S}_k\mathbf{V}_k^T \quad k \in (\mathbf{LL}, \mathbf{LLH}, \mathbf{HL}, \mathbf{HH}) \tag{10}$$

The watermarked image $\mathbf{W}$ is subjected to the key $\mathbf{SK}$-based Arnold transform to obtain the disordered watermarked image $\mathbf{W}^*$, and $\mathbf{W}^*$ is processed using a one-level DWT, which likewise yields a low-frequency approximation subband as well as three high-frequency detail subbands $\mathbf{W}_k$.

The matrix $\mathbf{C}$ is obtained by multiplicatively adding the singular values $\mathbf{S_k}$ corresponding to the obtained $\mathbf{Y}$ components with $\mathbf{W_k}$ according to the equation, respectively.

$$\mathbf{S_k} + \mathbf{Q_k}\mathbf{W_k} = \mathbf{C_k} \quad k \in (\mathbf{LL}, \mathbf{LH}, \mathbf{HL}, \mathbf{HH}) \tag{11}$$

Where $\mathbf{Q}$ is the embedding strength in the watermarking algorithm and the value is obtained by IWO algorithm.

The SVD inverse decomposition of the matrix $\mathbf{C}$ is performed and the luminance component $\mathbf{Y_w}$ of the image after the addition of the watermark is obtained using a three-level DWT inverse transform.

$$\mathbf{U_k}\mathbf{S_k}\mathbf{V_k}^{\mathrm{T}} = \mathbf{Y_{wk}} \quad k \in (\mathbf{LL}, \mathbf{LH}, \mathbf{HL}, \mathbf{HH}) \tag{12}$$

Finally, the luminance component $\mathbf{Y_w}$ is combined with the $\mathbf{I}$ and $\mathbf{Q}$ colour components in the $\mathbf{YIQ}$ format corresponding to image $\mathbf{A}$, and the $\mathbf{YIQ}$ format is converted to $\mathbf{RGB}$ format to finally obtain the watermarked image $\mathbf{A_w}$.

4.3. **Watermark extraction algorithm.** The watermark containing image $\mathbf{A}^*_{\mathbf{w}}$ after attack is subjected to colour space conversion, $\mathbf{RGB}$ is converted to $\mathbf{YIQ}$ format and $\mathbf{Y_w}$ component is extracted.

The SVD decomposition of $\mathbf{Y_w}$ according to Equation (13) yields the matrices $\mathbf{U}^*$, $\mathbf{S_w}$, and $\mathbf{V}^{\mathrm{T}}$.

$$\mathbf{Y}'_{\mathbf{wk}} = \mathbf{U}'_{\mathbf{k}}\mathbf{S}'_{\mathbf{wk}}\mathbf{V}'\mathbf{T_k} \quad k \in (\mathbf{LL}, \mathbf{LH}, \mathbf{HL}, \mathbf{HH}) \tag{13}$$

The singular value $\mathbf{S}$ corresponding to the luminance component $\mathbf{Y}$ of image $\mathbf{A}$ and the singular value matrix $\mathbf{S_w}$ corresponding to the watermarked image (attacked) are computed according to Equation (14), and the matrix $\mathbf{W}^*$ can be obtained, where the embedding factor $\mathbf{Q}$ is kept constant.

$$\mathbf{W}'^*_{\mathbf{wk}} = (\mathbf{S}'_{\mathbf{wk}} - \mathbf{S_k})/\mathbf{Q_k} \quad k \in (\mathbf{LL}, \mathbf{LH}, \mathbf{HL}, \mathbf{HH}) \tag{14}$$

The matrix $\mathbf{W}'^*$ is inverted by one level of DWT to extract the disrupted watermark image $\mathbf{W}^*$ after the attack.

The extracted watermark image $\mathbf{W}^*$ can be obtained by performing the Arnold inverse transformation of $\mathbf{W}^*$ with the disruption number $\mathbf{SK}$.

4.4. **Specific steps for digital image watermarking.** The IWO based digital copyright protection method for colour images is shown in Algorithm 1.

The proposed method consists of three main parts: (1) reading the original colour image and watermarked image data; (2) initialising the invasive weed optimisation (IWO) algorithm parameters; and (3) initialising the watermark embedding parameters, such as watermark intensity, position, size, etc.

5. Experimental results and analyses.

5.1. **Experimental environment and experimental dataset.** In order to verify the performance of IWO algorithm in digital image watermarking, Matlab is used for example simulation. Particle swarm algorithm [19], differential evolutionary algorithm [20] and IWO algorithm are used for comparison respectively. Embedding strength in watermarking algorithm is obtained by differential evolutionary algorithm.

Set the target fitness value of IWO algorithm to 0.05, and its initial values are shown in Table 2.

Algorithm 1 IWO-based Digital Copyright Protection for Colour Images

```
// IWO algorithm parameter setting
population_size = 50 // population size
max_generation = 100 // maximum number of iterations
feature_dimension = width * height * channels // image feature dimension (size of the image and number of channels)
// Initialisation of populations
InitializePopulation(population_size, feature_dimension) // randomly initialise individuals in the population
// IWO algorithm main iteration process
for generation in 1 to max_generation do
    for each weed in population do
        EvaluateFitness(weed) // Evaluate fitness of each weed (individual)
        // Intrusion process - update based on fitness
        invasive = SelectInvasiveWeed(population) // select invasive weeds
        UpdateWeed(weed, invasive) // update current weed based on invasive weeds
        // Reproduction process - reproduction based on optimal weeds
        best_weed = SelectBestWeed(population) // select the most adapted weed
        Reproduce(weed, best_weed) // Reproduce using best weed
    end for
end for
// End Evaluation
// Getting the best weed (the most adapted weed)
best_weed = SelectBestWeed(population)
// Embedded Watermark - Optimised for IWO
EmbedWatermark(original_image, watermark_image, best_weed, watermark_strength, watermark_location)
// Output colour image with watermark
OutputWatermarkedImage(original_image)
// Watermark extraction
extracted_watermark = ExtractWatermark(original_image, watermark_location, watermark_size)
// Output extracted watermark
OutputExtractedWatermark(extracted_watermark)
```

The experimental watermark image is selected as a grey scale image of size 128×128. In order to better verify the reasonableness of the algorithm, two colour images both of size 512×512 are selected as carrier images, where Baboon image has more complex texture than Lena image. For better presentation, the size of the related images is appropriately adjusted. The dimension of the problem solved by the IWO algorithm is 4 since there are watermarks embedded in all four regions of the image transform domain.

Table 2. Initial value setting of IWO algorithm

$iter_{max}$	P_{max}	S_{min}	S_{max}	$\sigma_{initial}$	σ_{final}
200	46	1	6	1	0.0005

5.2. **IWO iterative performance verification.** In the research and application of optimization algorithm, the main purpose of iterative performance verification is to evaluate the efficiency and effectiveness of the algorithm. By verifying the iterative performance of the algorithm, the following information about convergence performance, stability and feasibility can be obtained. The optimal fitness value and the number of iterations are simulated and the results are shown in Figure 3.

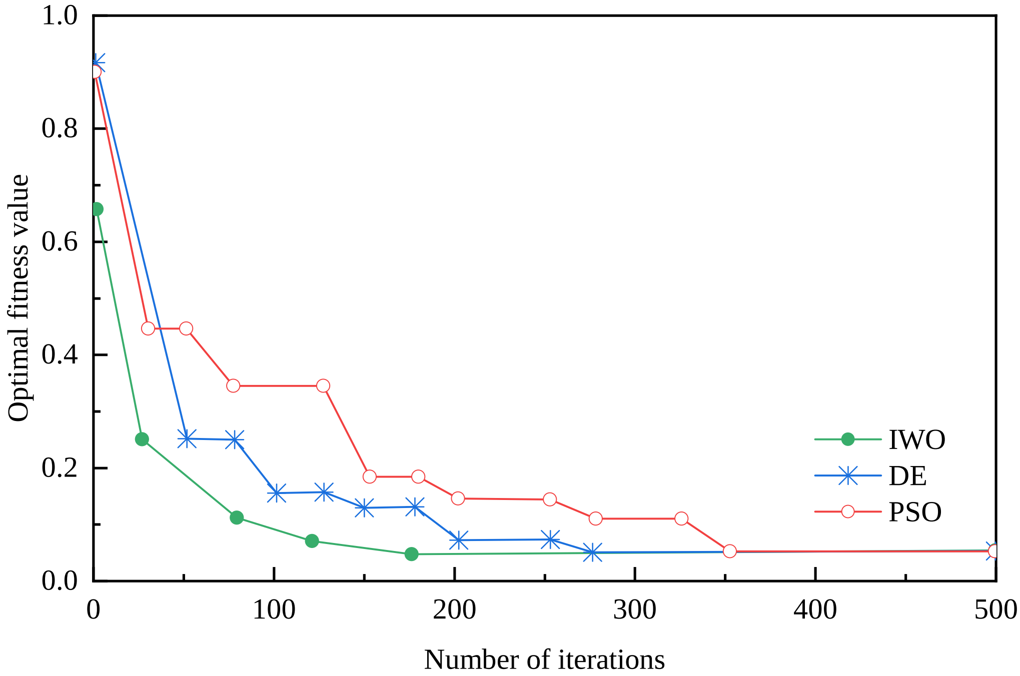

Figure 3. Convergence performance comparison

It can be seen that the IWO algorithm is optimal, obtaining the optimal fitness value in 52 iterations, whereas the DE algorithm reaches convergence in 108 iterations and the PSO algorithm reaches convergence in 142 iterations. From the convergence process, it can also be seen that the DE algorithm and PSO algorithm obtained the local optimal solution in 4 and 5 times respectively, while the IWO algorithm did not have a local optimal, which indicates that the IWO algorithm has an obvious advantage in terms of convergence performance.

5.3. **Watermark invisibility analysis.** Peak Signal to Noise Ratio (*PSNR*) is usually used to evaluate the image quality, but it can be used to assess the invisibility of the watermark or the effect of the watermark embedding on the original image. The invisibility of the watermark is evaluated based on the magnitude of the *PSNR* value.

PSNR is a metric used to compare the similarity between two images.It measures the visibility of the watermark by comparing the difference between the original image and the watermarked image. A higher value of *PSNR* indicates that the two images are more similar, thus indicating a higher level of invisibility of the watermark.The formula for calculating *PSNR* is shown below:

$$PSNR = 10 \cdot \log_{10}\left(\frac{Max^2}{MSE}\right) \tag{15}$$

Where Max denotes the maximum value of the image pixels (usually 255, for an 8-bit image) and MSE (Mean Squared Error) is the average of the squares of the pixel differences between the original image and the watermarked image.

Typically, if the *PSNR* value is high (close to the quality of the original image), it means that the watermark has better invisibility to the image. Conversely, if the *PSNR* value is low, it may mean that the watermark is more visible to the image. In general, when $PSNR > 30$, the modification of the image is not visible to the human eye, i.e., the reconstructed picture and the original image are hard to differentiate from one another.

The carrier image Lena and the carrier image Baboon are shown in Figure 4 and Figure 5, respectively. The watermark image is shown in Figure 6.

Figure 4. Carrier image Lena

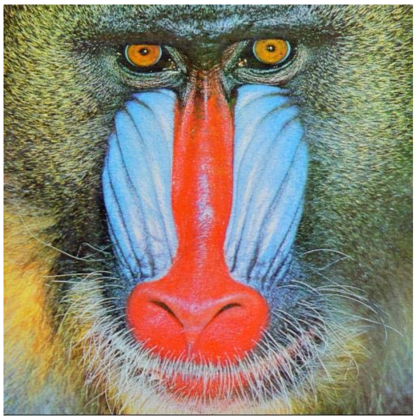

Figure 5. Carrier image Baboon

Figure 6. Watermarked images

Visually, the embedded watermark does not affect the carrier image, and the extracted watermark image is clearer and has high visual quality. In addition, the original watermark image can be extracted by calculating the PSNR values of the watermark-containing image and the carrier image as 46.2243 and 47.1536, respectively. In comparison to the original watermark image, the extracted watermark image has an NC value of 1. It can be proved that the IWO watermarking algorithm can effectively ensure the concealment of the image embedded watermark, i.e., the algorithm has good invisibility.

5.4. **Watermarking Robustness Analysis.** In the robustness experiments, the watermark-containing images are attacked separately by Gaussian noise (0.03), pretzel noise (0.04), clipping (top left 1/4, bottom right 1/4), counterclockwise rotation (20°, 40°), JPEG compression (8, 12, 65, 90), and panning (60×60, -60×60). Figure 7 and Figure 8 show the watermark-containing images of the clipping attack. Figure 9 and Figure 10 shows the watermarked image extracted after the attack.

Figure 7. Watermarked image Lena

Figure 8. Watermarked image Baboon

Figure 9. Extracted watermark Lena

Figure 10. Extracted watermark Baboon

Through visual observation, it can be found that the watermark image extracted after the attack and the original watermark image have different degrees of changes in sensory quality, but can still be clearly distinguished. The features of the extracted watermark image are clearer. In addition, in order to objectively verify the robustness of the algorithm, the correlation of the experimentally obtained watermarked images is compared and examined by calculating the NC value between the extracted watermarked image and the original watermarked image. The comparison folds of NC values between the extracted watermarked image and the original watermarked image under different attack methods are shown in Figure 11.

It can be seen that in different attack methods and under different parameters, the NC values of the extracted watermarked images obtained by the IWO algorithm and DE

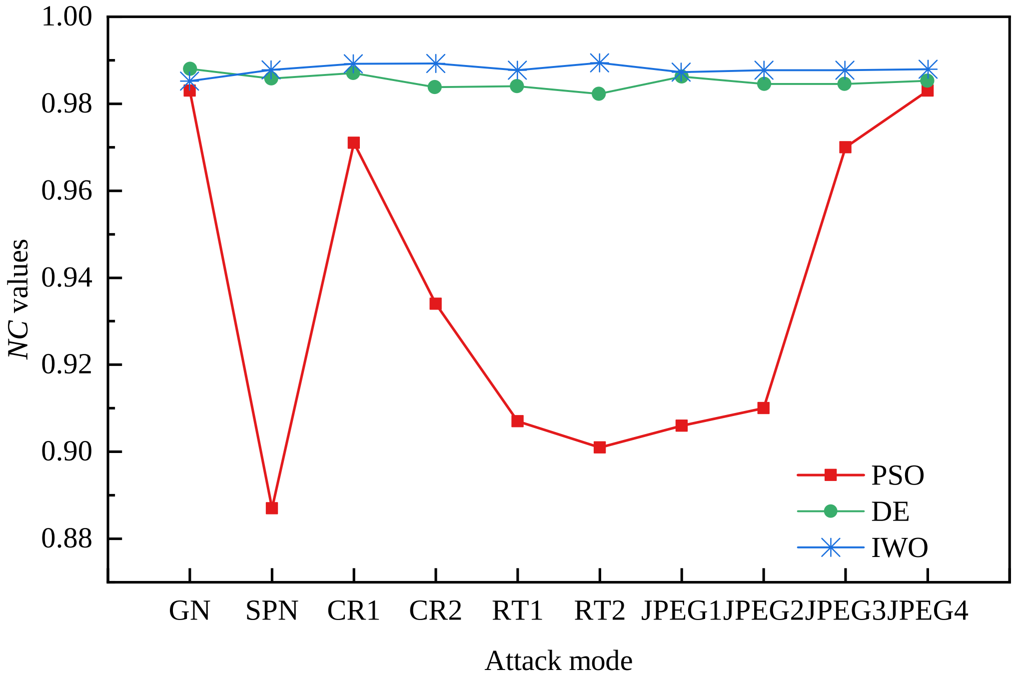

Figure 11. Comparison of NC values obtained by different watermarking algorithms

algorithm do not differ much from the original watermarked image, and the NC values are above 0.95 and the variation is small. While PSO algorithm has more fluctuation and obvious disorder such as SPN, RT1, RT2, JPEG1 and JPEG2.Therefore, the colour image watermarking algorithm based on IWO algorithm shows high robustness.

6. **Conclusion.** In this work, an image digital copyright protection technique based on invasive weed optimisation algorithm is proposed. Firstly, the principles and characteristics of the human visual system are introduced, and the perceptual characteristics of colour images and the conversion relationship between colour spaces are analysed. Then, the proposed watermarking algorithm is described in detail, in which the watermarked image is disordered to increase the security of the algorithm. Secondly, the colour image is used as the carrier image of the watermarking algorithm, and the appropriate watermark embedding intensity is selected based on the IWO algorithm in combination with the HVS characteristics. It not only increases the applicability of the algorithm, but also shows strong robustness to noise attacks, compression, and geometric attacks such as rotation, shear, and translation on the basis of ensuring certain algorithmic invisibility. However, the population diversity maintenance of IWO can be further improved. A better diversity maintenance strategy can help the algorithm better avoid falling into local optimal solutions. Follow-up studies will be conducted to analyse this issue.

REFERENCES

[1] Y. Zhou, C. Huang, Q. Hu, J. Zhu, and Y. Tang, "Personalized learning full-path recommendation model based on LSTM neural networks," Information Sciences, vol. 444, pp. 135-152, 2018.
[2] H. Peng, S. Ma, and J. M. Spector, "Personalized adaptive learning: an emerging pedagogical approach enabled by a smart learning environment," Smart Learning Environments, vol. 6, no. 1, pp. 1-14, 2019.

[3] H. Xie, H.-C. Chu, G.-J. Hwang, and C.-C. Wang, "Trends and development in technology-enhanced adaptive/personalized learning: A systematic review of journal publications from 2007 to 2017," Computers & Education, vol. 140, 103599, 2019.

[4] M. L. Bernacki, and C. Walkington, "The role of situational interest in personalized learning," Journal of Educational Psychology, vol. 110, no. 6, 864, 2018.

[5] O. Rudovic, J. Lee, M. Dai, B. Schuller, and R. W. Picard, "Personalized machine learning for robot perception of affect and engagement in autism therapy," Science Robotics, vol. 3, no. 19, eaao6760, 2018.

[6] I. H. Sarker, A. Kayes, and P. Watters, "Effectiveness analysis of machine learning classification models for predicting personalized context-aware smartphone usage," Journal of Big Data, vol. 6, no. 1, pp. 1-28, 2019.

[7] R. M. Martins, and C. Gresse Von Wangenheim, "Findings on teaching machine learning in high school: A ten-year systematic literature review," Informatics in Education, vol. 22, no. 3, pp. 421-440, 2023.

[8] T.-Y. Wu, A. Shao, and J.-S. Pan, "CTOA: Toward a Chaotic-Based Tumbleweed Optimization Algorithm," Mathematics, vol. 11, no. 10, 2339, 2023.

[9] T.-Y. Wu, H. Li, and S.-C. Chu, "CPPE: An Improved Phasmatodea Population Evolution Algorithm with Chaotic Maps," Mathematics, vol. 11, no. 9, 1977, 2023.

[10] T.-Y. Wu, Q. Meng, S. Kumari, and P. Zhang, "Rotating behind Security: A Lightweight Authentication Protocol Based on IoT-Enabled Cloud Computing Environments," Sensors, vol. 22, no. 10, 3858, 2022.

[11] A. L. H. P. Shaik, M. K. Manoharan, A. K. Pani, R. R. Avala, and C.-M. Chen, "Gaussian Mutation–Spider Monkey Optimization (GM-SMO) Model for Remote Sensing Scene Classification," Remote Sensing, vol. 14, no. 24, 6279, 2022.

[12] M. Samiullah, W. Aslam, M. A. Khan, H. M. Alshahrani, H. Mahgoub, A. M. Abdullah, M. I. Ullah, and C.-M. Chen, "Rating of Modern Color Image Cryptography: A Next-Generation Computing Perspective," Wireless Communications and Mobile Computing, vol. 2022, pp. 1-20, 2022.

[13] I. Vasiljevic, R. Obradovic, I. Duric, B. Popkonstantinovic, I. Budak, L. Kulic, and Z. Milojevic, "Copyright protection of 3D digitized artistic sculptures by adding unique local inconspicuous errors by sculptors," Applied Sciences, vol. 11, no. 16, 7481, 2021.

[14] R. Sinhal, D. K. Jain, and I. A. Ansari, "Machine learning based blind color image watermarking scheme for copyright protection," Pattern Recognition Letters, vol. 145, pp. 171-177, 2021.

[15] K. J. Giri, and R. Bashir, "A block based watermarking approach for color images using discrete wavelet transformation," International Journal of Information Technology, vol. 10, pp. 139-146, 2018.

[16] M. H. Vali, A. Aghagolzadeh, and Y. Baleghi, "Optimized watermarking technique using self-adaptive differential evolution based on redundant discrete wavelet transform and singular value decomposition," Expert Systems with Applications, vol. 114, pp. 296-312, 2018.

[17] L. Salimi, A. Haghighi, and A. Fathi, "A novel watermarking method based on differential evolutionary algorithm and wavelet transform," Multimedia Tools and Applications, vol. 79, no. 17-18, pp. 11357-11374, 2020.

[18] F. N. Thakkar, and V. K. Srivastava, "Performance comparison of recent optimization algorithm Jaya with particle swarm optimization for digital image watermarking in complex wavelet domain," Multidimensional Systems and Signal Processing, vol. 30, pp. 1769-1791, 2019.

[19] Z. Zheng, N. Saxena, K. Mishra, and A. K. Sangaiah, "Guided dynamic particle swarm optimization for optimizing digital image watermarking in industry applications," Future Generation Computer Systems, vol. 88, pp. 92-106, 2018.

[20] X. Cui, Y. Niu, X. Zheng, and Y. Han, "An optimized digital watermarking algorithm in wavelet domain based on differential evolution for color image," Plos One, vol. 13, no. 5, e0196306, 2018.

[21] Y. Zhuang, S. Liu, C. Ding, and X. Zhou, "Reversible watermarking based on extreme prediction using modified differential evolution," Applied Intelligence, vol. 52, no. 12, pp. 14406-14425, 2022.

[22] A. Bose, and S. P. Maity, "Secure sparse watermarking on DWT-SVD for digital images," Journal of Information Security and Applications, vol. 68, pp. 103255, 2022.

[23] S. Kumar, D. R. Parhi, K. K. Pandey, and M. K. Muni, "Hybrid IWD-GA: an approach for path optimization and control of multiple mobile robot in obscure static and dynamic environments," Robotica, vol. 39, no. 11, pp. 2033-2060, 2021.

[24] P. Sivananthamaitrey, and P. R. Kumar, "Performance analysis of meta-heuristics on dual watermarking of color images based on SWT and SVD," Multimedia Tools and Applications, pp. 1-27, 2022.

[25] X. Yue, and H. Zhang, "A multi-level image thresholding approach using Otsu based on the improved invasive weed optimization algorithm," Signal, Image and Video Processing, vol. 14, pp. 575-582, 2020.
[26] A. A. Movassagh, J. A. Alzubi, M. Gheisari, M. Rahimi, S. Mohan, A. A. Abbasi, and N. Nabipour, "Artificial neural networks training algorithm integrating invasive weed optimization with differential evolutionary model," Journal of Ambient Intelligence and Humanized Computing, pp. 1-9, 2021.
[27] M. Misaghi, and M. Yaghoobi, "Improved invasive weed optimization algorithm (IWO) based on chaos theory for optimal design of PID controller," Journal of Computational Design and Engineering, vol. 6, no. 3, pp. 284-295, 2019.
[28] W. Wang, G. Tian, G. Yuan, and D. T. Pham, "Energy-time tradeoffs for remanufacturing system scheduling using an invasive weed optimization algorithm," Journal of Intelligent Manufacturing, pp. 1-19, 2021.
[29] B. S. Halbhavi, S. Kodad, S. Ambekar, and D. Manjunath, "Enhanced invasive weed optimization algorithm with chaos theory for weightage based combined economic emission dispatch," Journal of Computational Mechanics, Power System and Control, vol. 2, no. 3, pp. 19-27, 2019.
[30] N. Rathod, and S. Wankhade, "Optimizing neural network based on cuckoo search and invasive weed optimization using extreme learning machine approach," Neuroscience Informatics, vol. 2, no. 3, 100075, 2022.
[31] E. Mohammed Abdelkader, O. Moselhi, M. Marzouk, and T. Zayed, "Hybrid Elman neural network and an invasive weed optimization method for bridge defect recognition," Transportation Research Record, vol. 2675, no. 3, pp. 167-199, 2021.